Design of gain-scheduling cascade control for a motion compensated gripper frame

Schepers, J. M.; Fidalgo Domingos, D. A.; Ter Braak, J.; Van Winsen, I.; Van Wingerden, J. W.

PAPER • OPEN ACCESS

Design of gain-scheduling cascade control for a motion compensated gripper frame

To cite this article: J M Schepers *et al* 2022 *J. Phys.: Conf. Ser.* **2265** 032082

View the article online for updates and enhancements.

Design of gain-scheduling cascade control for a motion compensated gripper frame

J M Schepers[1,2], D A Fidalgo Domingos[1], J ter Braak[2], I van Winsen[2] and J W van Wingerden[1]

[1] Department of System and Control, TU Delft, Mekelweg 2, Delft 2628 CD, NL
[2] Heerema Engineering Solutions, Paardenmarkt 1A, Delft 2611 PA, NL

E-mail: `jobschepers@me.com`, `d.a.fidalgodomingos@tudelft.nl`,
`jterbraak@hes-heerema.com`, `ivanwinsen@hes-heerema.com` and
`j.w.vanwingerden@tudelft.nl`

Abstract. The offshore wind market is growing, resulting in larger wind turbines being installed farther away from the coast and into deeper waters. This trend brings challenges to an industry strongly depending on the use of jack-up vessels. A floating vessel equipped with a Dynamic Positioning (DP) system and a Motion Compensated Gripper Frame (MCGF) provides a more efficient solution to guide XXL monopoles during the installation phase. According to strict regulations, the offset angle of monopiles shall not be over 0.25^o. To ensure this, a robust control method is required to deal with gradual change in soil stiffness, wave induced motions and sensor delays. The control force exerted by the gripper frame can significantly affect the floating vessel dynamics, hence, this should be optimized.

Therefore, the research goal is to analyse the system and design a robustly stable control for the MCGF. In the context of this research, cascade PID control with gain-scheduling is chosen, which is able to control the Gripper Frame during all installation steps for different soil stiffness and to reject wave disturbances.

With the use of the lumped multiplicative uncertainty structure, the changing and uncertain soil-characteristics are modelled. The sensor delay to measure the monopile inclination, has a significant impact on system stability. Robust stability criteria are validated using the Nyquist criterion and by analysing the system's closed-loop poles. With the use of gain-scheduling it is possible to switch control settings during the installation. Time-domain results show that with this design approach the installation criteria are met such as the maximum monopile angle and the applied control force.

Ultimately, it is shown that robust PID control with gain-scheduling for a MCGF can ensure safe, efficient and cost-effective installation of the next generation wind turbines. Future research should focus into the definition and implementation of the gain-scheduling switching criteria.

1. Introduction

Due to an increased demand for renewable and sustainable forms of energy, the wind industry is growing rapidly [1]. Wind energy is one of the most promising green energy sources and has been growing ever since the first wind turbine was installed [2]. Especially the offshore wind parks are growing in interest since onshore space is scarce and political choices are based on visual pollution and noise disturbances [3]. New wind turbines are becoming larger in size and are placed further offshore in order to make wind energy more cost-effective [1]. Wind parks further

offshore in deeper waters make the installation more challenging. The current methodology uses a jack-up vessel, however this methodology is less suited for installing the next generation of XXL wind turbines in deeper waters. Jack-up vessel are slow and the length of the legs limit their offshore operating area. Floating vessels with a Dynamic Positioning (DP) system are able to operate in deeper waters and claim to be more time efficient [4].

A Motion Compensated Gripper Frame (MCGF) is needed to control the position and angle of a monopile during installation when using a DP vessel. Figure 1 shows the installation steps and the different elements of the model. The challenge arises in compensating the first and second order vessel motions and wave disturbance on the monopile with this gripper frame. The gripper motions are limited in x-y direction. In [5] a numerical model of the coupled system of the monopile and vessel is established. Also in [6] time-domain simulations were carried out to study the installation process of a monopile, including lowering phase, landing phase and steady states after landing. So multiple studies have already been done on analyzing monopile vessel interactions and dynamics. However, within this research the focus is on the controller design of a MCGF. Some of the major challenges of the control design for this new installation method are stated below. The DP system of the vessel actively compensates for the wave forces on the vessel and compensates second order motions of a vessel. Motions of the monopile and offsets of the vessel position by this DP system make it challenging to compensate these by the gripper frame. Another challenge occurs in the changing properties of the soil, due to different soil layers and increase of penetration depth in the soil during the installation. Soil properties expressed by its stiffness will change over penetration depth and at every position within a wind farm. So when a monopile is installed and the penetration depth increases, the stiffness of the monopile and gripper frame interaction will change over time. Suitable control methods to deal with these challenges are MPC, H-infinity [7] and LQR [8] which are all model based, however larger deviations within the model can be tolerated with the use of PID control. Therefore gain scheduling with a PID controller is considered as the most suitable approach for designing the controller for a MCGF. PID controllers are defined as robust controllers and are able to deal with larger model uncertainties.

This paper describes the design of the controller of this MCGF, to control the angle and position of the XXL monopile during the installation. The system is described by a linear model of the vessel, monopile, MCGF and is affected by disturbances by wave force on the vessel and the monopile. Within limits this linear models is a valid approximation of the dynamics. A robust cascade PID controller is tuned which can deal with model uncertainty and is able to gain-schedule for the different operating models.

2. Objectives

The foundation of a windturbine needs to be installed within an inclination tolerance of $\pm 0.25^o$ [9]. The soil stiffness changes over time and for different sea bed types, therefore this parameter is defined as $Ksoil \in [Ksoil_{min}, Ksoil_{max}]$. The robust controller should be able to deal with this uncertainty range. Moreover, the wave forces on the monopile and vessel motions cause periodic disturbances within the system which the controller should be able to reject. The mean resulting force and maximum control force of the MCGF should be minimised since these forces effect the vessel positioning. A mean constant force on the vessel can cause unstability of the DP system, since it will push away the vessel. Which in the end will cause the vessel to drift from its original position, resulting in the gripper frame to reach its extension limits.

The research goal can be classified as follows; design a robust stable PID controller which is able to control the MCGF and stabilize the monopile during all installation scenarios for the different degree of soil stiffness, while optimizing the required control force. The objective of the controller of the gripper frame is to minimise the deviation and the maximum of the inclination
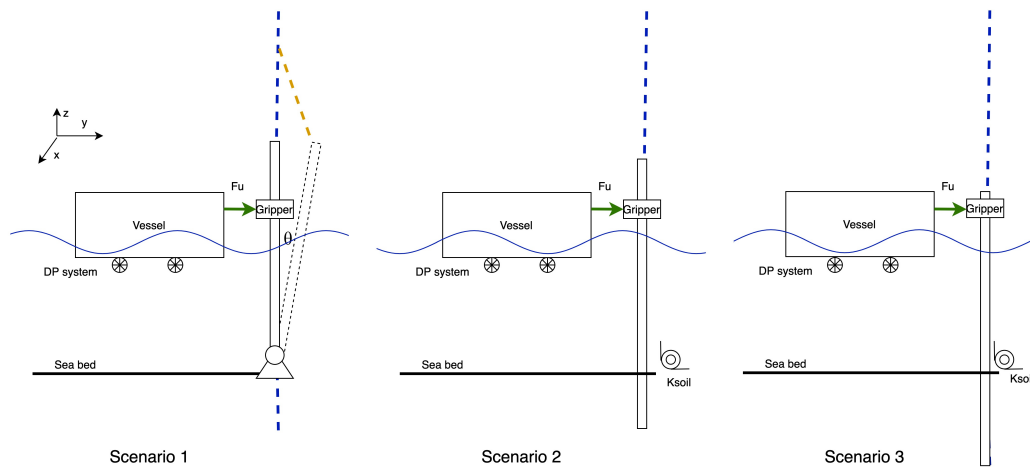
Figure 1: Installation steps and schematic overview of the model, consisting of the vessel with an active DP system, the gripper frame and the monopile soil interaction. Scenario 1 the monopile is unstable, scenario 2 is marginally stable and scenario 3 is stable.

angle θ [degr] during the installation. The control input of the system is expressed by the used force F_u[kN], which can also be expressed by the power $P_{gripper}$ [kWh] required by the gripper frame and both parameters should be minimised. The constraints of the system within this research are a maximum control force of $F_u = 3600\ kN$, a maximum gripper acceleration of $a_{gf} = 4.5\ m/s^2$ and the gripper frame has an extension limit of ± 3 m. One of the most important system parameters in this research is the soil stiffness, $Ksoil$ [kN/rad], it influences the natural frequency ω [rad/s] of the system. Resonance may occur whenever the natural frequency of the system matches with the frequency of the wave disturbance, this effect should always be avoided. Hence, the objective of the controller is to have a larger bandwidth then the frequency of the disturbances. The objectives and research goal have been elaborated, the constraints are set and the most important parameters which influence system dynamics have been discussed. Next, is the methodology to describe the steps of this research to design a robust stable PID controller.

3. Methodology
This research uses a linear model which consists of the gripper frame, the vessel and the monopile as illustrated in Figure 1. The equation of motions are determined based on a Free Body Diagram (FBD) of the model, the interaction between different states of the system can be expressed by transfer functions. A monopile can show rigid and flexible mode shapes during installation. For simplicity a linear model is used assuming rigid behaviour of the monopile. Poulos [10] has formulated a definition for rigid or flexible behavior of a monopile which could be used for further research. The monopile in this research has a length of 108 m, weight of 2300 mT and a diameter of 11 m. Different theories exist in the literature regarding modelling the soil interaction [11], [12], [13]. This research uses a rotational spring to express the soil stiffness and therefore leaves out the lateral spring effects. The dynamics of the model are illustrated in the scheme of Figure 2, in which $G(s)$ is the transfer function of the stiffness and damping of the gripper, $R(s)$ is the transfer function of the ring in the MCGF and $M(s)$ is the transfer function of the monopile based on the sum of moment around the contact point at the seabed. The transfer function of the plant consists of the relation between input F_u and the output θ. The plant (Figure 2) has two negative feedback loops, first the transfer function from x_g to θ is computed, the derivation

can be found in the Appendix A, and is given by:

$$M_c(s) = \frac{\theta}{x_g} = \frac{M(s)l_g R(s)}{1 + M(s)R(s)l_g^2} \tag{1}$$

The transfer function from F_u to x_g is derived from the control scheme in Figure 2 and equals:

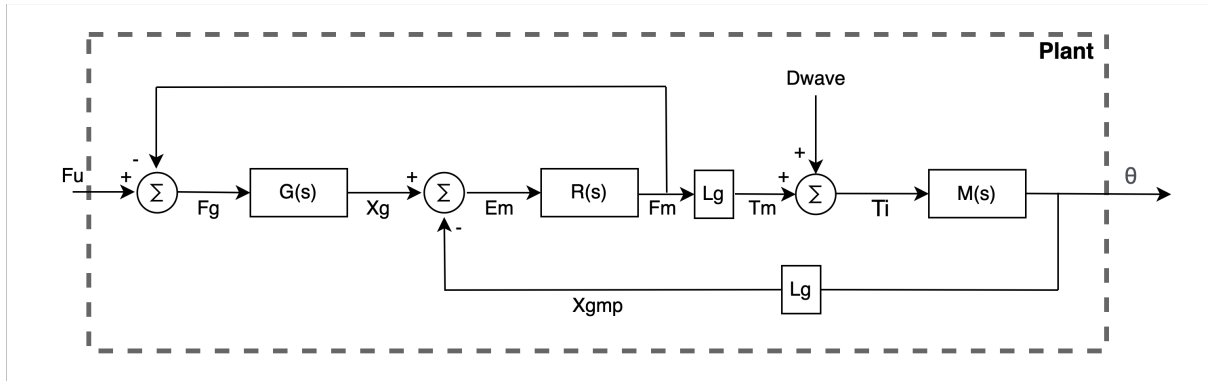$$M_u(s) = \frac{x_g}{F_u} = \frac{G(s)}{1 + G(s)R(s)(1 - M_c(s)l_g)} \tag{2}$$

Figure 2: The scheme of the physical interaction between the components of the model. The Gripper, Ring and the Monopile are described by the transfer functions $G(s), R(S)$ and $M(s)$. The variable Lg is the height of the gripper compared to the seabed. E_m is the error between the gripper position x_g and the position x_{gmp} caused by the linear angle offset $\theta \cdot l_g$. τ_m is the moment applied by the Ring on the monopile, this is summed with the wave disturbance resulting in τ_i. The plant (dashed box) is describing the dynamics from the input F_u to the output θ.

Then finally the plant $P(s)$ is described by,

$$P(s) = \frac{\theta}{F_u} \tag{3}$$

$$P(s) = M_c(s)M_u(s) \tag{4}$$

$$P(s) = \frac{M_c(s)G(s)}{1 + G(s)R(s)(1 - M_c(s)l_g)}. \tag{5}$$

As discussed in the objective the changing soil stiffness affects the natural frequency of the system. The natural frequency is defined by, $\omega(s) = \sqrt{\frac{Ksoil}{I_{mp}}}$, in which I_{mp} is the moment of inertia of the monopile and $Ksoil$ the changing soil stiffness. This uncertainty and variance affects the transfer function $M(s)$ and therefore $P(s)$. The plant is based on the transfer function between the input F_u and the output θ with a soil stiffness between the defined operating points: $Ksoil1$ = 0 kNm/deg to $Ksoil4 = 7486000$ kNm/deg. This results in a natural period of the system between 2 to 24 seconds, depending on the soil stiffness and monopile moment of inertia.
Wave forces which disturb the system are simulated by using the JONSWAP spectrum with a significant wave height of 2.4 m and a peak period of 7 s, this disturbance enters the system at D_{wave} in Figure 2. Whenever the natural frequency of the system corresponds to the wave period, additional damping and a high bandwidth is required within the controller to be faster

than the disturbances.

Measurement sensors are used for the position of the vessel, the position of the gripper frame and the angle of the monopile. The sensors are modelled using predefined accuracy's and delays. The current state-of-the-art inclination sensor has a delay of 0.5 seconds which is limiting the maximum possible bandwidth of the controller when using this sensor. The vessel used within this research is the semi-submersible vessel Balder from Heerema with a DP system. The vessel dynamics are described by mass spring damper transfer functions in surge and yaw direction. The parameters of added mass and additional damping are frequency dependent. For simplifications, in this research the parameter values are used corresponding to the frequency of the peak period of the wave disturbance.

The designed cascade control scheme is illustrated in Figure 3. The plant from Figure 2 is simplified in the control scheme and indicated by $P(s)$. In order to deal with Delay3 of $\tau = 0.5(s)$ of the inclination sensor a cascade control strategy is designed with a faster inner-loop controller. The delay of 0.5 s results in theoretical maximum bandwidth of 2 seconds which is proven to be not robustly stable. The cascade controllers are tuned in time and frequency domain, based on settling time, rise time and magnitude of the sensitivity function $(S(s))$ and the complementary sensitivity function $(T(s))$. The inner-loop $C2(s)$ PID is tuned on the dynamics of the gripper frame position x_g, described by transfer function $M_u(s)$. The outer-loop $C1(s)$ PD controller controls the set point of the inner-loop. A feedforward controller $C_{FF}(s)$ based on the vessel velocity sensor is implemented which rejects the disturbance caused by the vessel motions: DX_v. [14] describes the design of a robust stable cascade PD-PID controller. The inner-loop controls the absolute position of the gripper x_g while the outer loop controls low frequent motions of the monopile θ. The system and control methodology have now been discussed, next is modeling the uncertainty within the system and validating the robust stability.

Modelling uncertainty Lumped multiplicative uncertainty structure is used to model the uncertainty in the plant, caused by the variance in soil stiffness and uncertainties within the soil stiffness [15]. The perturbed plant $G_p(s)$ is modelled, as [16]

$$G_p(s) = P(s)\left(1 + w_I(s)\Delta_I(s)\right); \quad |\Delta_I(j\omega)| \le 1 \forall \omega$$
$$L_p(s) = C(s)G_p(s)$$

The weight w_I represents the magnitude of the uncertainty in frequency-domain, $\Delta(s)$ is any stable transfer function of which the magnitude is less or equal than 1 for all frequencies [16]. $L_p(s)$ is the perturbed open-loop transfer function.

Robust stability validation The robust stability of the designed controllers is validated for the plants with the uncertainty sets based on the Nyquist criterion and analysing the system closed-loop poles [16], as illustrated in Figure 4a for operating point $Ksoil3$. The black dotted lines show the magnitude of relative uncertainty per frequency. The blue line is the designed uncertainty bound described by the weight w_I which indicates the magnitude of the uncertainty at each frequency. Figure 4b shows the Nyquist curve not crossing through the critical point -1 and Figure 4c shows the poles of the closed-loop perturbed system which are all in the LHP.

The distance of the Nyquist curve to the point of -1 equals $|1 + L|$. The region of the disc represents L_p and the radius of the disc equals $|w_I L|$. Therefore L_p does not encircle -1 for [16]:

$$\text{RS} \Leftrightarrow |w_I L| < |1 + L|, \quad \forall \omega \Leftrightarrow \left|\frac{w_I L}{1 + L}\right| < 1, \forall \omega$$
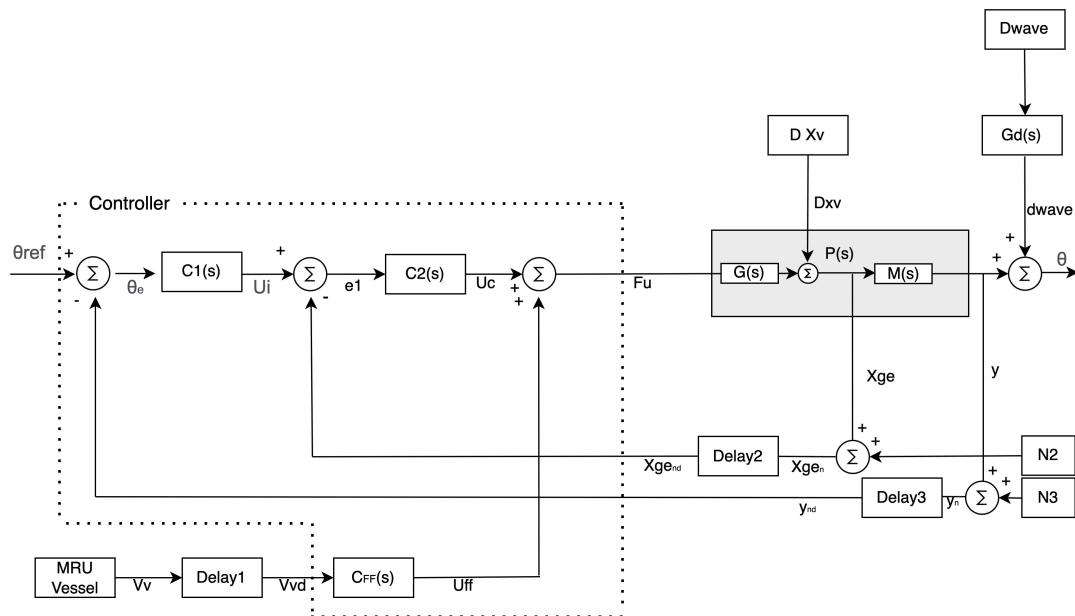
Figure 3: The inner-loop controller $C1(s)$ controls the state x_g with control output u_c, while the outer-loop Ci measure the output θ and sets the reference value for the inner-loop with control output u_i. The error e_1 is the offset which needs to be compensated by the inner-loop. The disturbance by the vessel position is compensated by the Feed Forward (FF) controller $C_{ff}(s)$, with control signal u_{ff}. The delay and noise caused by the two sensors is taken into consideration in this control design.
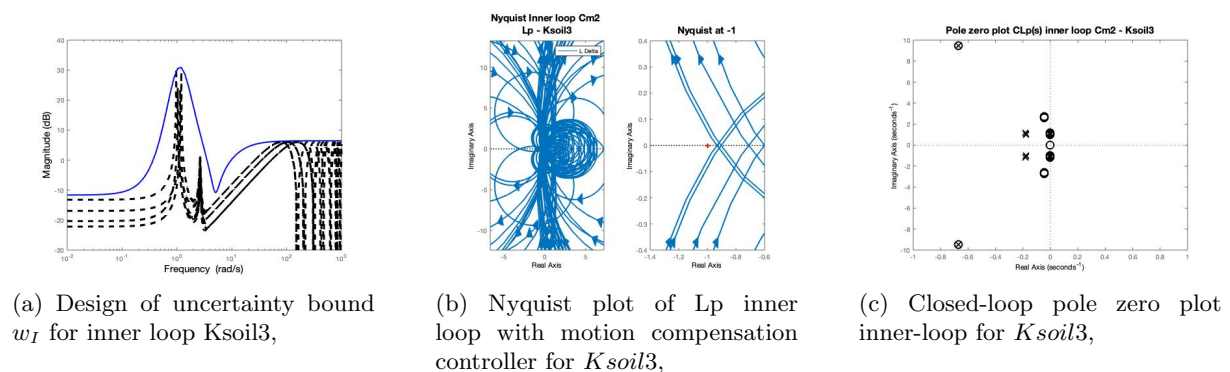

(a) Design of uncertainty bound w_I for inner loop Ksoil3,

(b) Nyquist plot of Lp inner loop with motion compensation controller for $Ksoil3$,

(c) Closed-loop pole zero plot inner-loop for $Ksoil3$,

Figure 4: Showing the robust stability analysis for the inner-loop controller for operating point $Ksoil3$.

However, the circle indicating the uncertainty range $L_p(s)$ is wider and covers a larger frequency spectrum than the real perturbations do indicated by the black crosses, as illustrated in Figure 5. The uncertainty of the system at critical frequencies $\omega = 30$ rad/s are shown to be close to the Nyquist curves instead of deviating within the circled uncertainty areas and moving to the critical point -1. This result support the fact that a circle used to express the uncertainty region is conservative in this particular case.
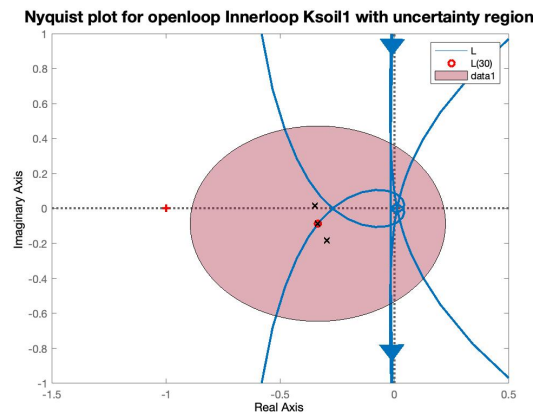
Figure 5: Nyquist curve for the inner loop Ksoil1 at $(j\omega)$ with the highest uncertainty, the circle regions is the uncertainty region given by $|Lw_I|$ which can be interpreted as conservative compared to the perturbations indicated by the black X.

Different gain settings of the PD and the PID controller are used to derive a robustly stable controller for the different operating points. Gain-scheduling is implemented to smoothly switch between the controllers for the different operating points [17]. Any bumps in the control law during switching cause non-efficient and possible dangerous behaviour of the system [18]. The papers [19] and [20] propose mixing two or more algorithms' outputs. The "weight" of each control law depends on the distance from the current process's operating point. This approach is implemented within this research and uses a continuous interval between [0-1] to change between the computed control laws. The soil stiffness is modelled to increase over time, simulating the monopile being hammered into the seabed, this effect is shown in Figure 6. The green dotted lines indicate the switching points of the gains of the cascade controller. A time-domain simulation is used to validate the performances of the designed controller.
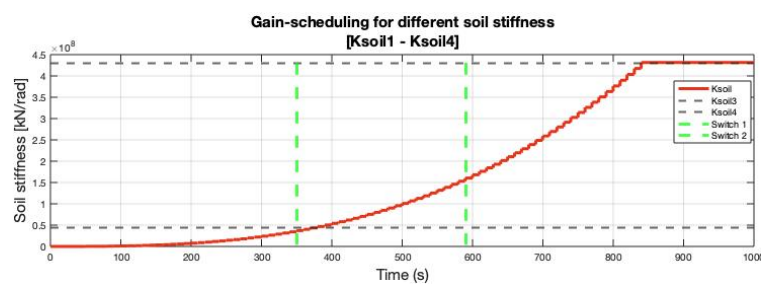
Figure 6: The increase in soil stiffness over time is shown in red. The black dotted horizontal lines show operating point $Ksoil3$ and $Ksoil4$. The green vertical dotted lines show the chosen switching points for gain-scheduling.

4. Results

The optimal controller is activated for the different operating points using gain-scheduling. The performance of the designed cascade controller is expressed using a time-domain simulation. In this simulation, wave forces are exerted as a disturbance on the monopile and vessel position. The soil stiffness and penetration depth is increased during the simulation. The designed controller

controls the output θ and the position of the gripper x_g with control force F_u. The simulation in Figure 7 shows the result for using a controller with 3 gain-scheduling controllers. The output does not violate the maximum angle of $\theta = 0.25^o$ ($\theta_{max} = 0.224^o$ and $\sigma(\theta) = 0.041^o$), moreover the control force is within its bounds of $F_u < 3600\ kN$ and the gripper acceleration does not exceed $4.5\ m/s^2$. An increase in monopile motion is shown in the time window between 300 and 400 seconds. At this point in time the peak frequency of the wave energy corresponds with the natural frequency of the system due to the changing soil stiffness. More damping is required within the controller, after scheduling the gains at switching point 1 the the frequency and magnitude of θ starts to diminish.
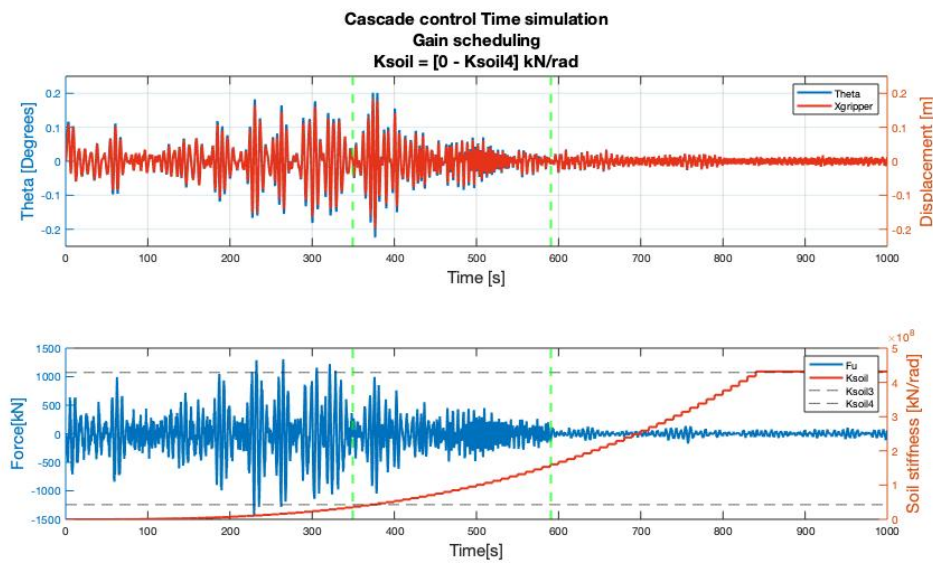

Figure 7: Result of time simulation, the top figure left y-axis shows the output θ plotted in blue, the right y-axis shows the displacement of the gripper x_g and is plotted in red. The bottom figure, shows the applied control force F_u on left y-axis and is plotted in blue, the increase in soil stiffness $Ksoil$ is plotted in red and shown on the right y-axis.

The designed cascade controller is robustly stable and the inner-loop controller has a 10 times higher bandwidth than a designed single-loop inclination controller. This has to do with the faster sensor in the inner-loop and with tuning of the control gains. The inner-loop of the cascade controller is designed for multiple purposes; a high and a low frequent motion controller in order to deal with the wide range of degree of soil stiffness. The performances of the inner-loop controller meet the objectives set for frequency and time-domain. Also, the constraints of the system are not violated, such as maximum force, velocity and acceleration of the gripper frame. The designed outer-loop is again limited by the delay of the inclination sensor.
The robust stability analysis show the designed cascade controllers are robustly stable for the perturbed plants. The used method could lead to an unstable scenario for an uncertainty within the set which is not modelled. However, there are results that show that the parametric uncertainties modelled with a circle region is conservative.

This research also analysed the effect of a change in sea state and different patterns of soil stiffness. The designed controllers are able to deal with a sea state with wave periods between 5.5 seconds and 8.5 seconds. For a shorter peak period the waves disturbance will affect with the system at a higher soil stiffness. The moment of switching is critical, and hence has a large influence on the performance of the MCGF.

5. Conclusions

The results provided in this research, within the assumptions used, support the use of gain-scheduling PID cascade control with multiple controllers. With the design method proposed in this research a robust stable cascade PID controller can be designed for a MCGF. A single-loop inclination controller was shown not to be robustly stable for specific operating points. The results show a stable system for all the changing degrees of soil stiffness. To better understand the implications of these results, future studies could address on when to switch between the different models and increase the reality of the study by implementing a 3-D model. In this research switching between the models and controllers is time triggered. Implementing a state observer enables to observe the states of the system which can not be measured. Based on this estimate or other measurement signals a suitable controller can be chosen. This would increase the overall performance and reality of the designed controllers.

Another approach to describe uncertainty regions compared to the one used in this research is the use of polytope regions. The regions can be described by an arbitrary set that needs to contain 0, which is can also be a polytope [21]. This is not taken into further consideration within this research but can improve the design approach.

Overall, the implementation of control strategy in the installation of offshore wind industry is promising. With this research the offshore wind industry is better capable of facing the challenges which arise during the design of a controller for a MCGF for offshore XXL monopiles. The developed method is the next step to installing the next generation XXL wind turbines in deeper waters, and replaces the current limited method which uses jack-up vessels. Using the designed cascade gain-scheduling controller will result in a robust stable controller which is able to fast and safely install the next generation of XXL monopiles. Hence, the cost of installing monopiles can be reduced even further which increases the speed of the energy transition.

Appendix A

Derivation of transfer function of system

Transfer function of $M_c(s)$

$$\theta(s) = M(s)l_g R(s)(x_g(s) - l_g\theta(s)) \tag{6}$$

$$\theta(s)(1 + M(s)l_g^2 R(s)) = M(s)l_g R(s)x_g(s) \tag{7}$$

$$\theta(s) = \frac{M(s)l_g R(s)}{1 + M(s)R(s)l_g^2}x_g(s) \tag{8}$$

$$M_c(s) = \frac{\theta}{x_g} = \frac{M(s)l_g R(s)}{1 + M(s)R(s)l_g^2} \tag{9}$$

Transfer function of $M_u(s)$

$$x_g(s) = G(s)(F_u(s) - R(s)(x_g(s) - l_g\theta(s))) \tag{10}$$

$$x_g(s) = G(s)(F_u(s) - R(s)(x_g(s) - l_g M_c(s)x_g(s))) \tag{11}$$

$$x_g(s) = G(s)(F_u(s) - R(s)x_g(s) + R(s)l_g M_c(s)x_g(s)) \tag{12}$$

$$x_g(s) = G(s)F_u(s) - G(s)R(s)x_g(s) + G(s)R(s)l_g M_c(s)x_g(s) \tag{13}$$

$$x_g(s)(1 + G(s)R(s) - G(s)R(s)l_g M_c(s)) = G(s)F_u(s) \tag{14}$$

$$x_g(s) = \frac{G(s)}{1 + G(s)R(s)(1 - M_c(s)l_g)}F_u(s) \tag{15}$$

$$M_u(s) = \frac{x_g}{F_u} = \frac{G(s)}{1 + G(s)R(s)(1 - M_c(s)l_g)} \tag{16}$$

References

[1] WindEurope. Offshore wind in Europe Key trends and statistics 2019. *Refocus*, 3(2):14–17, 2019.

[2] M. Dolores Esteban, J. Javier Diez, Jose S. López, and Vicente Negro. Why offshore wind energy? *Renewable Energy*, 36(2):444–450, 2011.

[3] Andrew R. Henderson, Colin Morgan, Bernie Smith, Hans C. Sørensen, Rebecca J. Barthelmie, and Bart Boesmans. Offshore wind energy in europe - A review of the state-of-the-art. *Wind Energy*, 6(1):35–52, 2003.

[4] L.G. Buitendijk. *Floating installation of offshore wind turbine foundations - Van Oord*. PhD thesis, 2016.

[5] Lin Li, Zhen Gao, Torgeir Moan, and Harald Ormberg. Analysis of lifting operation of a monopile for an offshore wind turbine considering vessel shielding effects. *Marine Structures*, 39:287–314, 2014.

[6] Lin Li, Zhen Gao, and Torgeir Moan. Numerical Simulations for installation of offshore wind turbine monopiles using floating vessels. *Proceedings of the ASME 32th International Conference on Ocean, Offshore and Arctic Engineering OMAE2013*, 32:1–11, 2013.

[7] Dengying and Zhoujie. LPV H-infinity controller design for a wind power generator. In *2008 IEEE International Conference on Robotics, Automation and Mechatronics, RAM 2008*, pages 873–878. IEEE, 9 2008.

[8] Adrian Ilka and Vojtech Vesely. Robust LPV-based infinite horizon LQR design. *Proceedings of the 2017 21st International Conference on Process Control, PC 2017*, 21:86–91, 2017.

[9] DNV GL. Support structures for wind turbines. *DNV GL - Standard*, 4:40–45, 2016.

[10] H Poulos and T Hull. The Role of Analytical Geomechanics in Foundation Engineering. 1989.

[11] A. H. Augustesen, K. T. Brødbæk, M. Møller, S. P.H. Sørensen, L. B. Ibsen, T. S. Pedersen, and L. Andersen. Numerical modelling of large-diameter steel piles at Horns Rev. *Proceedings of the 12th International Conference on Civil, Structural and Environmental Engineering Computing*, 12(91):1–14, 2009.

[12] Caselunghe Aron, Eriksson Jonas, Aron Caselunghe, and Jonas Eriksson. *Structural Element Approaches for Soil-Structure Interaction*. PhD thesis, 2012.

[13] Mingchao Wang, Yongsheng Zhao, Weikang Du, Yanping He, and Ruhong Jiang. Derivation and validation of soil-pile-interaction models for offshore wind turbines. *Proceedings of the International Offshore and Polar Engineering Conference*, 9:181–188, 2013.

[14] R. Vilanova and O. Arrieta. PID tuning for cascade control system design. *Canadian Conference on Electrical and Computer Engineering*, (1):1775–1778, 2008.

[15] S. P. H. Sørensen and A. H. Augustesen. Small-displacement soil-structure interaction for horizontally loaded piles in sand. *Geotechnical structures and infrastructure*, 17:775–786, 2016.

[16] Sigurd Skogestad and Ian Postlethwaire. *Multivariable Feedback Control: Analysis and Design*. 2005.

[17] Ahmed A.M. Hakim and Ibrahim M.H. Sanhoury. Adaptive Control for x Inverted Pendulum Utilizing Gain Scheduling Approach. *International Conference on Computer, Control, Electrical, and Electronics Engineering, (ICCCEEE)*, pages 1–6, 2018.

[18] Ciprian Lupu, Pierre Borne, and Dumitru Popescu. Multi-model Adaptive Control Systems. *Control Engineering AND Applied Informatics*, 10(1):49–56, 2008.

[19] M. Dussud, S. Galichet, and L. Foulloy. Fuzzy Supervision for Continuous Casting Mold Level Control. *IFAC Management and Control of Production and Logistics*, 33:1137–1142, 2000.

[20] Kumpati S. Narendra and Jeyendran Balakrishnan. Improving Transient Response of Adaptive Control Systems using Multiple Models and Switching. *IEEE Transactions on Automatic Control*, 39(9):1861–1866, 1994.

[21] Carsten W. Scherer. *Theory of Robust Control*. 2001.